Journal of Cellular Biochemistry 92:1180–1192 (2004)

In Situ Non-Invasive Spectral Discrimination Between Bone Cell Phenotypes Used in Tissue Engineering

Ioan Notingher,[1]* Gavin Jell,[1] Ulrich Lohbauer,[1] Vehid Salih,[2] and Larry L. Hench[1]

[1]Department of Materials, Imperial College London, South Kensington Campus, London SW7 2BP, United Kingdom
[2]Department of Biomaterials, Eastman Dental Institute, University College London, London WC1X 8LD, United Kingdom

Abstract Raman micro-spectroscopy was used to discriminate between different types of bone cells commonly used in tissue engineering of bone, with the aim of developing a method of phenotypic identification and classification. Three types of bone cells were analysed: human primary osteoblasts (HOB), retroviral transfected human alveolar bone cells with SV40 large T antigen (SV40 AB), and osteoblast-like human osteosarcoma derived MG63 cell line. Unsupervised principal component analysis (PCA) and linear discriminant analysis (LDA) of the Raman spectra succeeded in discriminating the osteosarcoma derived MG63 cells from the non-tumour cells (HOB and SV40 AB). No significant differences were observed between the Raman spectra of the HOB and SV40 AB cells, confirming the biochemical similarities between the two cell types. Difference spectra between tumour and non-tumour cells suggested that the spectral discrimination is based on the fact that MG63 osteosarcoma derived cells are characterised by lower concentrations of nucleic acids and higher relative concentrations of proteins compared to the non-tumour bone cells. A supervised classification model (LDA) was built and showed high cross-validation sensitivity (100%) and specificity (95%) for discriminating the MG63 cells and the non-tumour cells, with 96% of the cells being correctly classified either as tumour or non-tumour derived cells. This study proves the feasibility of using Raman spectroscopy to identify in situ phenotypic differences in living cells. J. Cell. Biochem. 92: 1180–1192, 2004.

Key words: Raman spectroscopy; living cells; phenotypes; tissue engineering; PCA; LDA

Tissue engineering is a promising new alternative to the old methods of repairing or replacing diseased and damaged tissue. The principal idea in tissue engineering is to grow parts of tissues in vitro by culturing living cells on three-dimensional bioactive-bioresorbable scaffold materials. New bone can be grown in vitro by culturing bone cells on various biomaterials. Osteoblasts are central to the process of bone remodelling and are involved in many bone diseases. Primary osteoblasts obtained directly from patients are the ideal cells to study in vitro the interaction between bone cells and different biomaterials. However, the use of primary osteoblasts in vitro is sometimes limited because of difficulty in obtaining sufficient bone fragments for harvesting cells. Furthermore, primary osteoblasts are difficult to culture in vitro, have a finite life-span and also can lose their phenotype as the number of passages increases.

To overcome the limitations in using primary osteoblasts, many osteoblast-like cell lines have been developed. Osteosarcoma derived cell lines are relatively easy to culture and have a high rate of proliferation and long life-span. Such cell lines have been routinely used as a model for osteoblasts to characterise their interaction with various biomaterials [Kieswetter et al., 1996; Boyan et al., 1998; Fini et al., 2002; Blaker et al., 2003]. However, the major disadvantage of using osteosarcoma derived cell lines relates to whether the phenotype of these cells reflect

The study was performed at Department of Materials, Imperial College London, London, UK.

Grant sponsor: US Defence Advanced Research Projects Agency (DARPA); Grant number: N66001-C-8041.

*Correspondence to: Ioan Notingher, Department of Materials, Imperial College London, South Kensington Campus, London SW7 2BP, United Kingdom.
E-mail: i.notingher@imperial.ac.uk

Received 5 March 2004; Accepted 30 March 2004
DOI 10.1002/jcb.20136

the true phenotype of normal osteoblasts [Clover and Gowen, 1994; Bielbe et al., 1996]. Many studies have addressed the relevance of ostesarcoma derived cell lines to adult human biology and disease or in terms of their suitability for biochemical and molecular analyses. Phenotypic and biochemical similarities as well as differences between osteosarcoma derived cell lines and primary osteoblasts have been found, including the regulation of alkaline phosphatase, various cytokines, cytokine receptors, and growth factors [Clover and Gowen, 1994; Bielbe et al., 1996; Perez et al., 2003].

Immortalising primary bone cells by retroviral transfection is another method to obtain long term cultures of bone cells. The aim of this method is to design new cell-lines with biochemical properties as close as possible to primary osteoblasts. The SV40 T antigen is a recognised immortalising agent and has been used to obtain long life-span cell cultures from primary osteoblasts [Keeting et al., 1992; Bodine et al., 1996; Salih et al., 2001]. The phenotype of cell lines obtained by transfection is closer to the mature osteoblastic phenotype [Keeting et al., 1992; Bodine et al., 1996; Salih et al., 2001] since the biochemical abnormalities present in the osteosarcoma cell lines are absent.

Many biochemical methods are available to detect biochemical changes in cells that can be related to phenotypic modifications. Polymerase chain reaction (PCR), immunofluorescence, and immunochemistry are common biochemical methods used routinely for phenotypic characterisation of cells. Although these methods are rich in information and are able to provide specific and detailed biochemical characteristics of the cells, these methods are impossible to be applied in situ since they are invasive, require cell fixation, staining, or lysis. They also require many samples, long sample preparation times, and are expensive in terms of both labour and chemicals.

Raman spectroscopy is a well-established analytical tool and is based on the interaction of electromagnetic radiation with the sample molecules. A Raman spectrum represents a chemical fingerprint of the sample. This technique has three main advantages over conventional biological assays when applied to the study of living cells: (i) it is rapid (1–3 min per spectrum), (ii) it is non-invasive, thus no labels are required, (iii) no damage is induced to the cells if suitable laser wavelengths and powers are used [Puppels et al., 1991; Notingher et al., 2002], (iv) it is suitable for time course experiments because cells can be maintained in physiological conditions during the measurements (culture medium, temperature, CO_2).

Numerous applications of Raman spectroscopy to study tissues and cells have been reported. High-resolution Raman spectral studies were performed on cellular organelles, such as chromosomes [Puppels et al., 1990], cytotoxic vesicles in killer T lymphocytes [Takai et al., 1997], and cholesterol crystals in endothelial cells [Hawi et al., 1997]. The distribution of cellular components within living and fixed cells was imaged by using confocal Raman microscopes [Krafft et al., 2003; Uzunbajakava et al., 2003a,b]. Biochemical changes related to cell-cycle, cell death [Notingher et al., 2003; Verrier et al., 2004], and differentiation of embryonic stem cells, such as translation of RNA into proteins, have also been identified [Notingher et al., 2004a,b]. Formation and mineralisation of bone nodules in vitro have also been monitored using Raman micro-spectroscopy [Tarnowski et al., 2002; Gough et al., 2004].

Multivariate statistical methods of spectral analysis, such as principal component analysis (PCA) and linear discriminant analysis (LDA), have significantly contributed to the increase of application of spectroscopy to cancer detection [Stone et al., 2000, 2002; Haka et al., 2002; Koljenovic et al., 2002; Nijssen et al., 2002; Shafer-Peltier et al., 2002a; Crow et al., 2003; Kendall et al., 2003; Smith et al., 2003], chemical tissues imaging [Nijssen et al., 2002; Shafer-Peltier et al., 2002a,b; Kneipp et al., 2003], and discrimination and identification of microorganisms [Maquelin et al., 2000, 2003; Choo-Smith et al., 2001]. These statistical methods of processing spectral signatures are proven to be invaluable classification and prediction tools for comparing complex biological samples.

In this study, we compared the Raman spectra of three types of bone cells used in tissue engineering: human primary osteoblasts, retroviral transfected human alveolar bone cells with SV40 large T antigen, and osteoblast-like human osteosarcoma-derived cells (MG63 cell line). Various phenotypic aspects of MG63 and transfected alveolar bone cells, as well as their interaction with various scaffold materials, have been previously characterised [Clover

and Gowen, 1994; Bielbe et al., 1996; Kieswetter et al., 1996; Boyan et al., 1998; Salih et al., 2001; Fini et al., 2002; Blaker et al., 2003]. The study shows the feasibility of Raman spectroscopy to discriminate biochemical differences between different osteoblast cell types commonly used in tissue engineering. The final aim of this research is to develop this technique for in situ and non-invasive detection of phenotypic changes in osteoblasts cultured on bioactive scaffolds during bone growth in vitro.

MATERIALS AND METHODS

Cell Culture

Transfected human alveolar bone cells (SV40 AB) were a kind donation from V. Salih (Eastman dental institute, UCL, London). The cells were isolated, transfected, and characterised as previously described [Salih et al., 2001]. The human primary osteoblasts (HOB) were a kind donation from R. Biebly (Chelsea and Westminster Hospital, London, UK). The cells were isolated from the femoral head of 73-year-old male as previously described [Wergedal and Baylink, 1984]. All experiments were completed on HOB cells in their fifth passage. MG63 cells were isolated from a 14 year male with osteocarcinoma and obtained from ECACC (UK).

Exponentially growing cells were tested for viability (Trypan Blue dye exclusion assay (Invitrogen, Paisley, UK)) and seeded at approximately 2.5×10^4 cells/ml/well in a 48-well plate containing MgF_2 disks for 24 h. All cell types were cultures in DMEM supplemented with 10% foetal bovine serum, 1% L-Glutamine, 1% antibiotic-antimycotic, and 1% non-essential amino acids (all from Invitrogen) in a 5% CO_2 incubator at 37°C.

MgF_2 was the chosen substrate due to its low background signal and low solubility in water. To ensure that MgF_2 did not cause cell type specific changes, the morphology of the cells grown on MgF_2 and on culture plate plastic surfaces (NUNC^{TM}) were observed with an inverted microscope (Leica, Milton Keynes, UK) and compared. Scanning electron microscopy was also performed to determine the adhesion of osteoblasts on MgF_2 substrates. Cells were grown on MgF_2 substrates as previously stated, and fixed in 2.5% glutaldehyde (Sigma, Poole, UK) in phosphate buffered saline (PBS) for 40 min, followed by dehydration through an ethanol gradient (25–100%) and final washing in hexamethyldisilazan (Sigma) and mounting on carbon tape (M.E. Taylor Engineering, Rockville, MD). Prior to examination samples were placed in a vacuum for 30 min before gold coating and examination with a Jeol JSM 5610LV electron microscope. Ion dissolution studies were performed as Mg^{2+} and F^- ions may also have important consequences on cell behaviour. MgF_2 disks were placed in media (DMEM) for 24 and 72 h, after which the media was analysed with Inductively Coupled Plasma (ICP) Optical Emission Spectroscopy (Applied Research Laboratory 3580 B ICP analyser along with ICP Manager software (provided by Micro-Active Australia Pty Ltd.)) to obtain the elemental concentrations of Mg.

Since the fluoride ions cannot be detected by the ICP spectrometer, a proliferation MTT (3-(4,5-dimethylthiazole-2yl)-2,5-diphenyltetrazolium bromide) assay was performed to compare the metabolic activity of bone cells treated with the dissolution ions released by MgF_2 substrate and control untreated cells. Anova and Dunnet tests were performed to determine statistical significance.

Raman Spectral Measurements

The Raman spectra were measured using a Renishaw InVia spectrometer connected to a Leica microscope equipped with a water immersion objective ($63\times/NA = 0.9$). The beam from a 785 nm multi-element high power diode laser (≈ 120 mW at sample) was used for excitation. Step scans along the optical axis (z-axis) and over the edge of a sharp edge in lateral directions (x, y-axis) on a poly(dimethyl) siloxane (PDMS) sample were performed to determine the spatial resolution of the system: $\Delta z \approx 25$ μm, $\Delta y \approx 10$ μm, and $\Delta x \approx 5$ μm. The Raman spectrum of a cell was calculated as the average of four or five (depending on the shape of the cell) Raman spectra measured at the same height and different lateral positions in the cell at distances equal to half the resolution in the corresponding direction.

Twenty cells corresponding to each cell type were measured. Each Raman spectrum measured at a single location in a cell was integrated over 30 s. After correction for the spectral response of the spectrometer (a fluorescent green glass sample was used as reference), the Raman signal of PBS was subtracted using the method described by Maquelin et al. [2000]. For the PCA and LDA analyses, the second deriva-

tive spectra were used (Savitsky-Golay method, 21 points averaged, 2nd order polynomial fit), normalised using the standard normal variance method (for each spectrum the average of the intensities was set to zero and the standard deviation was set to one) [Wolthuis et al., 1999]. The standard deviation scaling factors of the second derivative spectra were used also for normalising the raw Raman spectra for the calculation of difference spectra.

A dataset of 60 Raman spectra was built with a total of 20 cells for each cell type. To ensure repeatability Raman spectra were collected on 3 separated days, with 3–4 cells/MgF_2 disc and 2–3 MgF_2 discs/day. The cells selected for measurements had an elongated morphology typical of healthy bone cells (as shown in Fig. 1).

The reference cellular components used in this study, calf thymus DNA and human serum albumin, were purchased from Sigma Ltd. (UK) and used without further purification. The Raman spectra were measured in PBS.

Data Analysis

PCA. PCA analysis finds combinations of variables that describe the major trends in the data [Wold et al., 1987]. This technique reduces the dimensionality of the measurement matrix with the goal to represent the data using smaller number of factors or principal components (PCs). The scores of Raman spectra corresponding to each PC were calculated as the projections of the Raman spectra on the directions defined by the PC loadings. The PCs retained for the analysis were the PCs that described the most significant variance between the spectra, while the less significant PCs, describing mostly random noise, were discarded.

The mean-centred Raman spectra of the cells were analysed using the PCA algorithm in PLS_Toolbox (Eigenvector Research, Inc., Mason, WA) and Matlab (MathWorks, Inc., Natick, MA).

LDA. PCA analysis is not the optimal method for spectral discrimination, because the PCA factors are computed to maximise the variance of the measurement matrix without considering sample groups. The LDA method is a powerful method for discrimination of sample groups. LDA computes linear combinations of variables to determine directions in the spectral space, discriminant functions (LDs), that maximise the variance between groups and minimise the variance within groups according to Fisher's criterion [Hair, 1998]. The main disadvantage of LDA is that the number of variables (wavenumber positions in a Raman spectrum) has to be smaller than the number of samples. Therefore, PCA was used as a data compression method and the most significant PCA scores were used as input to a LDA model [Wolthuis et al., 1999; Stone et al., 2002]. For the validation of the LDA model, the leave-one-out cross-validation method was used. In this method, all spectra except one were used to build a LDA model and then to classify the left out spectrum. This method is repeated so that each spectrum is predicted once. In-house

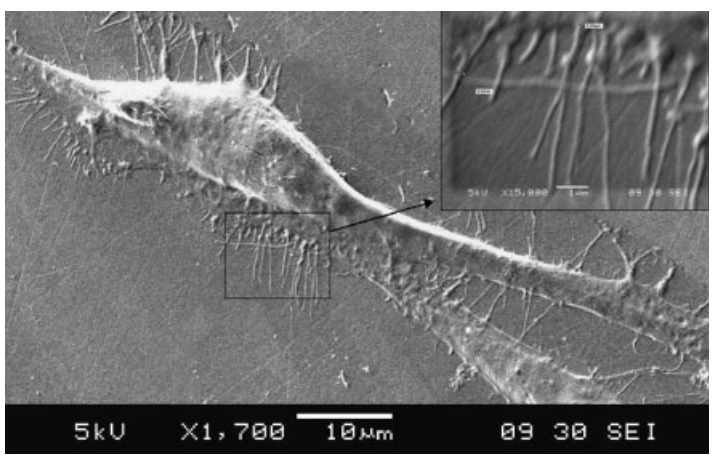

Fig. 1. Typical scanning electron micrograph (SEM) of a primary osteoblast grown on MgF_2 substrate. Note the characteristic elongated morphology and well-formed filopodia (insert) of a well-attached osteoblast.

software developed on Matlab platform (Mathworks, Inc.) was used for the calculation of the LDA scores and cross-validation.

RESULTS

Cell Morphology

Whilst it is widely accepted that the surface properties of a material, (i.e., chemistry and/or topography) can alter cell behaviour, cell attachment, morphology, and phenotype, no differences were observed in bone cell morphology between bone cells grown on MgF_2 compared with culture well plates. SEM analysis also revealed typical elongated osteoblast morphology with extended filopodia indicating good cellular attachment on the MgF_2 substrate (Fig. 1). It has been previously reported that Mg^{2+} has important roles in cellular process, including competing with Ca^{2+} binding sites [Koss and Grubbs, 1994]. However, Mg^{2+} ion release from MgF_2 in culture media was negligible with only 0.004 U/PPM detected after 24 and 72 h.

Previous studies also indicated that fluoride ions can inhibit the formation of pyruvate from glucose, which in turn reduces the mitochondrial activity causing ATP depletion [Niknahad et al., 1994; Jeng et al., 1998]. Since the ICP emission spectrometer was not sensitive to fluoride ions, a proliferation assay of the mitochondrial activity (MTT) was performed to compare bone cells treated with the culture media in which MgF_2 substrates were immersed for 24 h with control cells. No significant differences were observed in the proliferation rate of treated and control cells.

Following the morphological and proliferation assays, we concluded that the concentration of Mg^{2+} and F^- ions released in the culture medium by the MgF_2 substrates did not induce any negative effects on the bone cells.

Unsupervised PCA Analysis of Raman Spectra

The average normalised Raman spectra corresponding to primary osteoblasts, transfected alveolar bone cells, and osteosarcoma MG63 cells after the subtraction of PBS and optics background signals are shown in Figure 2A. The grey areas indicate ±standard deviation of the spectra. As expected, due to the relatively similar biochemical and phenotypic nature of the cells, there were only small cell type specific differences observed by Raman spectroscopy.

The Raman spectra of the bone cells in Figure 2A are similar to the published Raman spectra of other cell types [Puppels et al., 1990, 1991; Notingher et al., 2002, 2003, 2004a,b; Krafft et al., 2003; Uzunbajakava et al., 2003a,b] and consist of peaks corresponding to molecular vibrations of all cellular components, i.e., nucleic acids, proteins, lipids, and carbohydrates. Peak assignment of the Raman spectra based on published literature is given in Table I [Thomas and Hartman, 1973; Tu, 1982; Prescott et al., 1984; Gremlich and Yan, 2001].

The changes in the fluorescence background of the Raman spectra produced significant variance of the Raman spectra within the three groups. The second derivative of each Raman spectrum was calculated to eliminate the parabolic-like fluorescence background. This method significantly reduced the variance within the groups, as shown in Figure 2B.

Since the Raman peaks corresponding to different cellular components are overlapped and produce broad bands, the analysis of the very small spectral differences is difficult. Sensitive statistical methods were used to discriminate between the three cell phenotypes.

Initially, PCA analysis was performed on the mean-centred second derivative spectra. A leave-one-out cross-validation analysis showed only a small decrease in the root-mean-square error of cross-validation (RMSECV) after the fifth PC. Inspection of the covariance matrix eigenvalues suggested the first five PCs (47% of the total variance between the Raman spectra) would suffice for the analysis. The low signal-to-noise ratio in the higher PCA loadings supported this conclusion.

In order to find common cell type specific features in the Raman spectra, the scores of the PCs were analysed. The greatest discrimination between the cell types was observed in the PC1–PC2 and PC2–PC4 plans. The third and fifth PCs did not indicate any differences between the cell groups, therefore their scores are not discussed.

The plot of the first PC (PC1, 21.351% of variance captured) versus the second PC (PC2, 10.28% of variance capture) is presented in Figure 3A. Two main analytical clusters can be observed in the PC1 versus PC2 plot. One of the clusters is formed by the osteosarcoma MG63 cells while the second cluster is formed by the alveolar bone cells and the primary osteoblasts. No separation between the primary osteoblasts

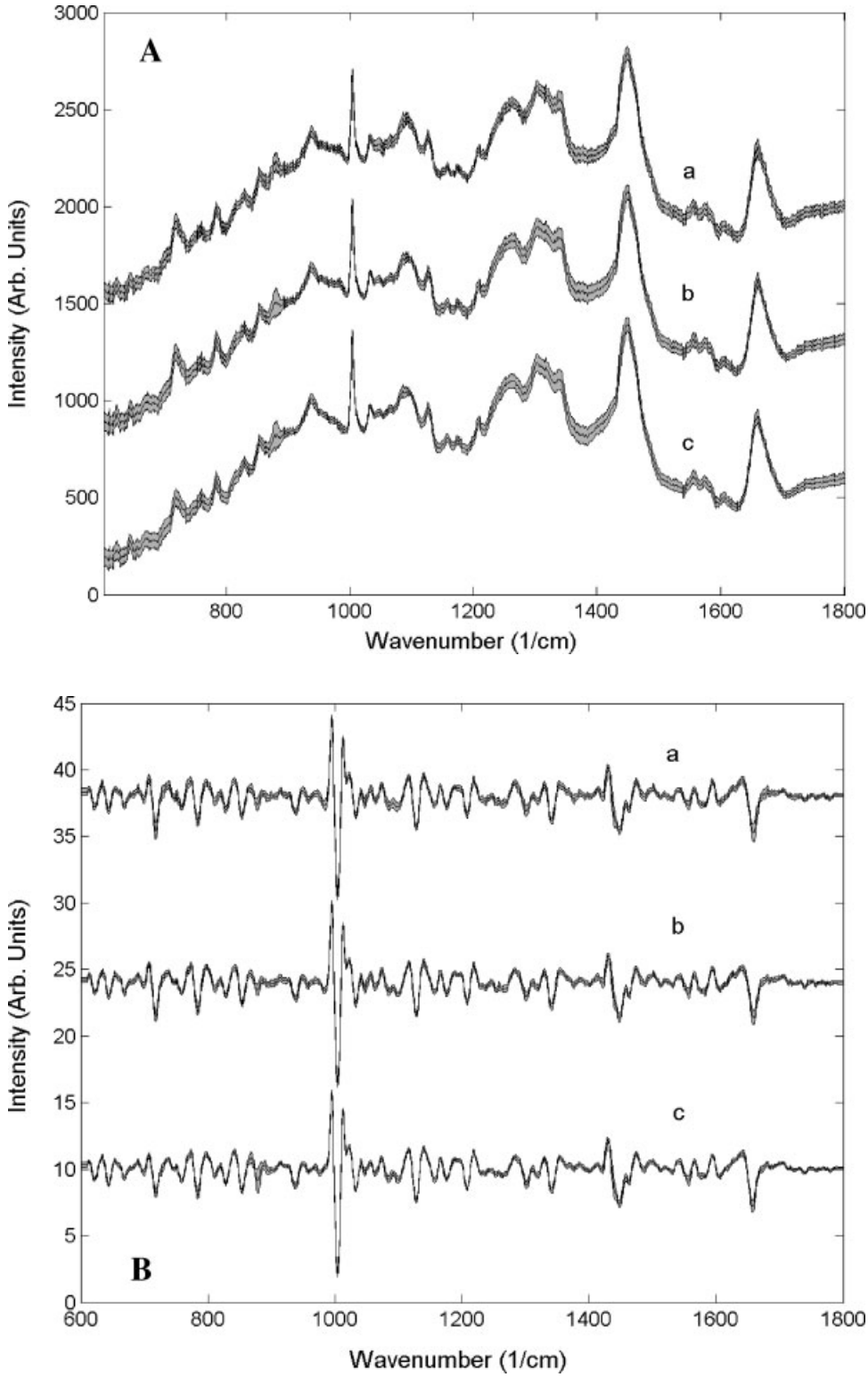

Fig. 2. Averaged and normalised Raman spectra (**A**) and 2nd derivative Raman spectra (**B**) of bone cells (middle black lines represent averages, grey areas represent +/− one standard deviation): (**a**) primary osteoblasts, (**b**) SV40 transfected alveolar bone cells, (**c**) MG63 osteosarcoma derived cells. For clarity, the Raman spectra were vertically shifted.

TABLE I. Assignment of the Major Peaks in the Raman Spectra of Bone Cells

	Assignment			
Peak (cm^{-1})	DNA/RNA	Proteins	Lipids	Carbohydrates
1,736			C=O ester	
1,680–1,655		Amide I	C=C str.	
1,617		C=C Tyr, Trp		
1,607		C=C Phe, Tyr		
1,578	G, A			
1,480–1,420	G, A, CH def	CH def	CH def	CH def
1,342	A, G	CH def		CH def
1,320	G	CH def		
1,301			CH_2 twist	
1,284–1,220	T, A	Amide III	=CH bend	
1,209		C-C_6H_5 str. Phe, Trp		
1,176		C-H bend Tyr		
1,158		C-C/C-N str.		
1,128		C-N str.		C-O str
1,095–1,060	PO_2^- str.		Chain C-C str.	C-O, C-C str.
1,033		C-H in-plane Phe		
1,005		Sym. Ring br Phe		
980		C-C BK str. β-sheet	=CH bend	
937		C-C BK str. α-helix	C-C-N^+ sym str	C-O-C glycos. bond C-O-C ring
877				
854		Ring br Tyr		
828	O-P-O asym.str.	Ring br Tyr		
811	O-P-O str. RNA			
788	O-P-O str. DNA			
782	U, C, T ring br			
760		Ring breath Trp		
729	A			
717			$CN^+(CH_3)_3$ sym str.	
667	T, G			
645		C-C twist Tyr		
621		C-C twist Phe		

and the transfected alveolar bone cells was observed. This indicates that the Raman spectroscopy can discriminate between the osteosarcoma derived MG63 cells versus non-tumour cells, but no significant biochemical differences were found among non-tumour cells.

Better separation between the tumour and non-tumour cells was observed when PC2 versus PC4 (4.03% variance captured) scores were plotted (Fig. 3B). The two analytical clusters of cells are well separated, which indicates that supervised patterned recognition models could be built to classify unknown cells as tumour derived or non-tumour cells.

Supervised LDA Classification Model

LDA analysis was used as a supervised pattern recognition technique to determine the ability to classify unknown bone cells on the basis of its Raman spectrum. A cell classification model was built to determine the accuracy of Raman spectroscopy to discriminate between the primary osteoblasts, alveolar bone cells, and MG63 cells.

The PCA scores on the two discriminating functions LD1 and LD2 were computed to produce maximum separation between the cell groups (Fig. 4). The tumour-derived and non-tumour cells were well separated along the LD1 direction, while only a slight non-significant separation between primary osteoblasts and alveolar bone cells was observed along the LD2 direction. The highest weights in the LD1 belonged to PC2 (−0.82) and PC4 (0.56), while LD2 was dominated by PC4 (0.86) and PC5 (0.43).

The accuracy of a prediction model based on PCA-LDA analysis of Raman spectra was tested using the cross-validation method (Table II). All 20 MG63 cells tested were correctly classified to belong to the MG63 group, indicating a sensitivity of 100%. Only two primary osteoblasts and no alveolar bone cells were predicted as belonging to MG63 class indicating a high specificity of the model (95%). Moreover, the PCA-LDA model showed that the biochemical differences between the primary osteoblasts and the alveolar bone cells were very small, confirming the biochemical similarity between the transfected alveolar bone cell-line and primary osteoblasts.

The total number of cells correctly classified was 70%, with most errors occurring due to misclassifications between primary osteoblasts

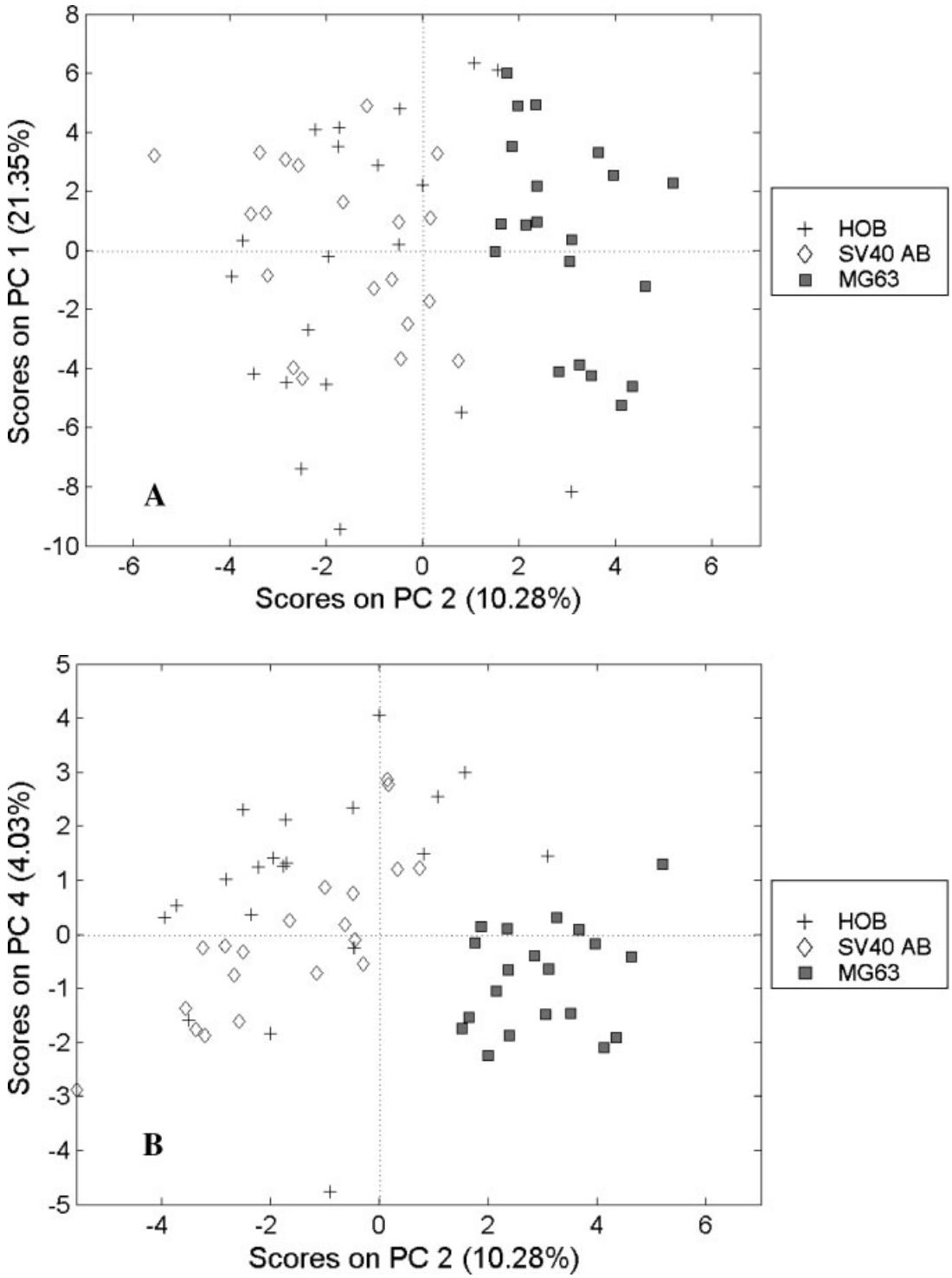

Fig. 3. Unsupervised principal component analysis (PCA) scores: PC1 versus PC2 (**A**), PC4 versus PC2 (**B**). Primary osteoblasts (HOB), SV40 transfected alveolar bone cells (SV40 AB), osteosarcoma derived cells (MG63).

and alveolar bone cells. When the classification was performed with only two groups, tumour versus non-tumour, 96.66% of the cells were correctly classified.

Analysis of Difference Raman Spectrum

Although the PCA and LDA techniques were able to discriminate between osteosarcoma

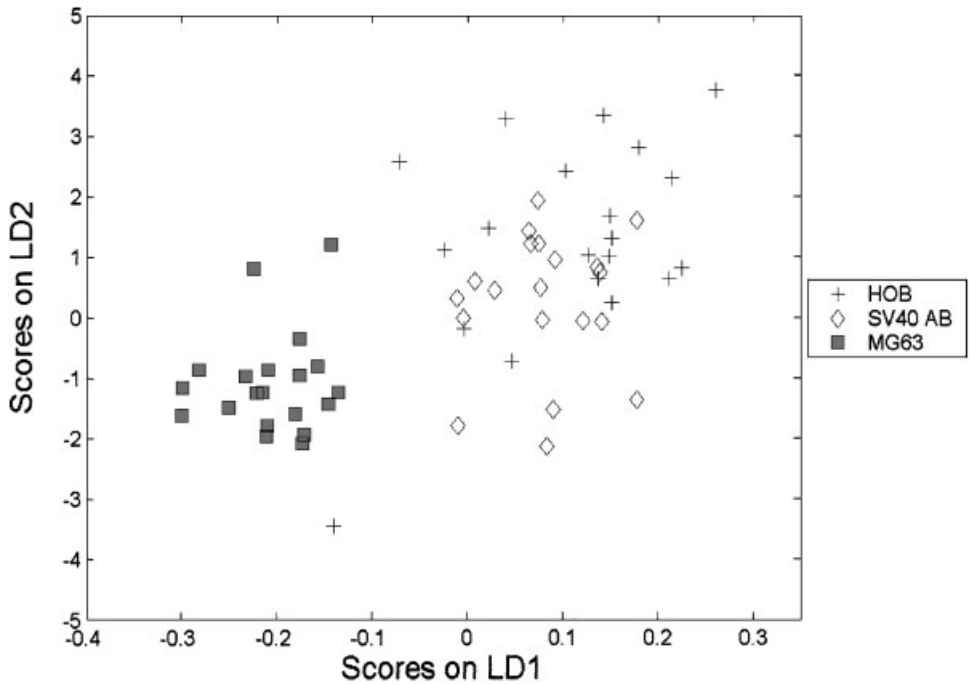

Fig. 4. LDA scores: HOB, SV40 AB, MG63.

MG63 cells and non-tumour bone cells, it is difficult to understand the biochemical differences on which the discrimination is based. The PCA loadings are abstract factors, with negative and positive peaks that are calculated in the PCA analysis in order to orthogonolise the loading and score vectors. Therefore, the loadings obtained in a PCA analysis of the Raman spectra of the bone cells are not the pure Raman spectra of individual biochemical components of the cells but rather combinations between the Raman spectra of the cellular components that vary between cells.

To identify the main biochemical differences, the difference between the average Raman spectra of primary osteoblasts and osteosarcoma-derived MG63 cells was computed and compared to reference Raman spectra of nucleic acids and proteins (Fig. 5). In the difference Raman spectrum, positive peaks corresponding to DNA (786 cm^{-1}: C, T, and O-PO backbone; 1,096 cm^{-1} PO_2^- backbone; 1,258 cm^{-1}, 1,345 cm^{-1}, 1,380 cm^{-1}, 1,578 cm^{-1}: A, G, T) and negative peaks corresponding to proteins (1,005 cm^{-1}: phenylalanine; 1,450 cm^{-1} C-H, 937 cm^{-1} C-C backbone) can be identified. This

TABLE II. Phenotype Classification Accuracy of the Raman Spectroscopy LDA Model by Leave-One-Out Cross-Validation Method

	Predicted phenotype by Raman[a]			
True classification	HOB	SV40 AB	MG63	Total
HOB	11	7	2	20
SV40 AB	9	11	0	20
MG63	0	0	20	20
Sensitivity	55%	55%	100%	
Specificity	77.5%	82.5%	95%	

HOB-human primary osteoblasts; SV40 AB-transfected alveolar bone cells; MG63-osteosarcoma MG63 cells.
[a]Percentage of cells correctly classified: 70%. When classification is made as tumour derived versus non-tumour cells, 96.66% of cells are correctly classified.

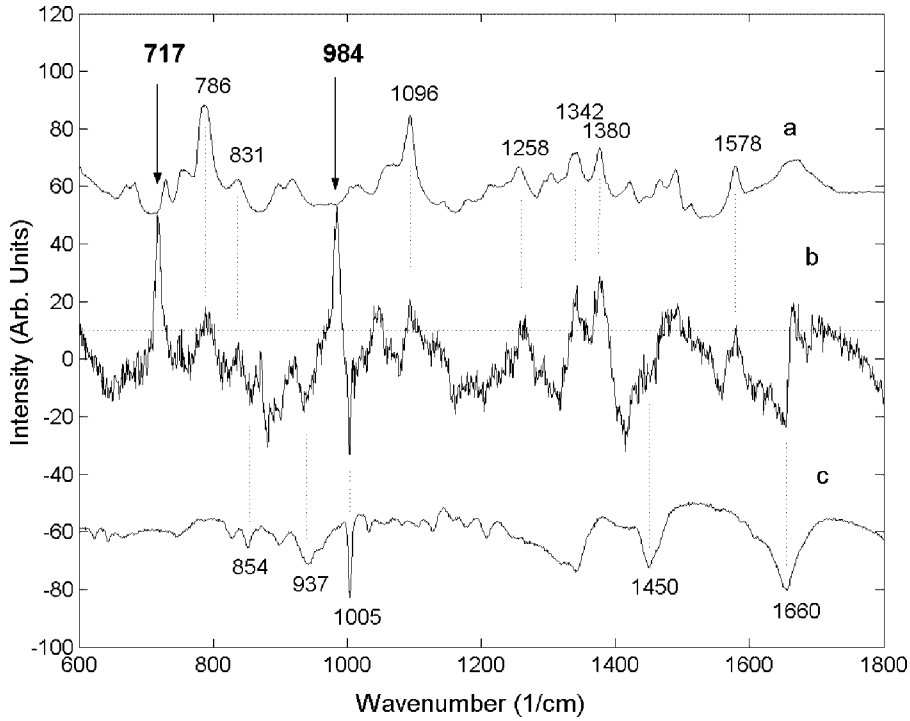

Fig. 5. Difference Raman spectrum between the average spectra of primary osteoblasts and osteosarcoma cells (**b**) compared to reference spectrum of DNA (**a**) and negative spectrum of proteins (**c**). Raman spectra are shifted vertically for clarity.

suggests that MG63 cells are characterised by lower concentrations of nucleic acid and higher concentrations of protein compared to non-tumour cells. These findings agree with previous reports using rat embryo fibroblasts transfected with the oncogene gene c-myc and untransfected unattached rat embryo fibroblasts in suspension [Omberg et al., 2002]. Cells with the oncogene gene had higher protein and lipid concentrations relative to DNA concentration [Omberg et al., 2002].

The conclusion that MG63 cells have lesser amounts of nucleic acids compared to non-tumour derived bone cells is somewhat surprising since tumour cells are thought to have higher concentrations of DNA as they proliferate more rapidly than non-tumour cells. This finding can be explained by the fact that the cells subjected to this study were selected to have a elongated morphology, specific to healthy bone cells, therefore the cells are very likely to be in G_0/G_1 phase of the osteoblast cell-cycle.

The difference Raman spectrum also indicated two high positive peaks: 717 and 984 cm^{-1}. The 717 cm^{-1} peak can be assigned to the $CN^{+}(CH_3)_3$ symmetric stretching vibrations of the choline group. However, research is ongoing for the identification of the chemical group responsible for the 984 cm^{-1} Raman peak.

DISCUSSION

This study shows that Raman micro-spectroscopy is a sensitive analytical technique to identify the phenotype of bone cells used in tissue engineering and indicates clear spectral differences between tumourigenic and non-tumourigenic cells. Combined with multivariate analysis methods, this technique could become an invaluable tool in the field of tissue engineering where there is a need for non-destructive real-time methods to characterise the phenotype of cells grown on biomaterials and in early detection of cancerous changes in cells.

The Raman spectra of three types of bone cells used in tissue engineering (human primary osteoblasts, retroviral transfected human alveolar bone cells with SV40 large T antigen, and osteoblast-like human osteosarcoma MG63 cell line) were measured to detect in situ biochemical differences between the three types of cells. Unsupervised PCA of the Raman

spectra of the cells succeeded in discriminating the tumour-derived MG63 cells from the non-tumour cells. No significant biochemical differences were observed between the Raman spectra of the retroviral transfected cell-line and the primary osteoblasts, suggesting that the two types of cells are very similar, which is consistent with the literature.

Further analysis of the PCA scores by LDA produced an even better separation between the cell groups. The classification accuracy of the PCA-LDA model was tested using the leave-one-out cross validation method. A clear distinction was made between the MG63 cells and the non-tumour cells (100% sensitivity and 95% specificity), with 96.66% of the cells being correctly classified. Despite the high discriminatory power of the PCA-LDA model, no significant differences were observed between the primary osteoblasts and the alveolar bone cells. This finding suggests that the retroviral transfected cells are biochemically closer to primary osteoblasts and therefore more suitable than osteosarcoma derived cell-lines for modelling the osteoblastic phenotype in tissue engineering and biomaterials compatibility studies. This biochemical detection method may also have important consequences in the rapid non-invasive detection of cancerous cells.

The calculated difference Raman spectrum indicated that MG63 osteosarcoma derived cells were characterised by higher relative concentrations of proteins and lower concentrations of nucleic acids compared to the non-tumour bone cells. These findings might be related to differences in cellular activity between the two cell groups.

The main advantage of this technology is that it allows monitoring the biochemical properties of the same cells over long periods of time. This study proved the feasibility of using Raman micro-spectroscopy and multivariate data analysis methods to detect small biochemical differences between cells in situ and it could be applied to other studies, such as differentiation and de-differentiation of cells, interaction between cells and drugs, toxic chemicals, substrate materials, or early detection of cancerous/abnormal cells in explants or in vitro studies. Future study is ongoing to determine whether the biochemical differences observed between primary and tumourigenic cells are specific to the type of cells studied or can be extrapolated to other cell types.

ACKNOWLEDGMENTS

The authors wish to thank Dr. Priya S Pavan for performing the ICP experiments.

REFERENCES

Bielbe G, Roberts E, Birch M, Evans DB. 1996. PCR phenotyping of cytokines, growth factors and their receptors and bone matrix proteins in human osteoblast-like cell lines. Bone 19:437–445.

Blaker JJ, Gough JE, Maquet V, Notingher I, Boccaccini AR. 2003. In vitro evaluation of novel bioactive composites based on Bioglass®-filled polylactide foams for bone tissue engineering scaffold. J Biomed Mater Res 67A: 1401–1411.

Bodine PVN, Trailsmith M, Komm BS. 1996. Development and characterisation of a conditionally transformed adult human osteoblastic cell line. J Bone Miner Res 11:806–819.

Boyan BD, Batzer R, Kieswetter K, Liu Y, Cochran DL, Szuckler-Moncler S, Dean DD, Scwartz Z. 1998. Titanium surface roughness alters responsiveness of MG63 osteoblast-like cells to 1 alpha,25-(OH)(2)(D-3). J Biomed Mater Res 39:77–85.

Choo-Smith L-P, Maquelin K, van Vreeswijk T, Bruining HA, Puppels GJ, Thi NA, Kirschner C, Naumann D, Ami D, Villa AM, Orsini F, Doglia SM, Lamfarraj H, Sockalingum GD, Manfait M, Allouch P, Endtz HP. 2001. Investigating microbial (micro)colony heterogeneity by vibrational spectroscopy. Appl Environ Microbiol 67:1461–1469.

Clover J, Gowen M. 1994. Are MG63 and HOS TE85 human osteosarcoma cell lines representative models of the osteoblastic phenotype? Bone 15:585–591.

Crow P, Stone N, Kendall CA, Uff JS, Farmer JA, Barr H, Wright MP. 2003. The use of Raman spectroscopy to identify and grade prostatic adenocarcinoma in vitro. Br J Cancer 89:106–108.

Fini M, Giavaresi G, Aldini NN, Torricelli P, Botter R, Beruto D, Giardino R. 2002. A bone substitute composed of polymethyl-methacrylate and alpha-tricalcium phosphate: Results in terms of osteoblast function and bone tissue formation. Biomaterials 23:4523–4531.

Gough JE, Notingher I, Hench LL. 2004. Osteoblast attachment and mineralzed nodule formation onrough and smooth 45S5 bioactive glass monoliths. J Biomed Mater Res 68A:640–650.

Gremlich HU, Yan B. 2001. Infrared and Raman spectroscopy of biological materials. New York: Marcel Dekker, Inc.

Hair JF. 1998. Multivariate data analysis. London: Upper Saddler River.

Haka AS, Shafer-Peltier KE, Fitzmaurice M, Crowe J, Dasari RR, Feld MS. 2002. Identifying microcalcifications in benign and malignant breast lesions by probing differences in their chemical composition using Raman spectroscopy. Cancer Res 62:5375–5380.

Hawi SR, Nithipatikom K, Wohlfeil ER, Adar F, Campbell WB. 1997. Raman microspectroscopy of intracellular cholesterol crystals in cultured bovine coronary artery endothelial cells. J Lipid Res 38(8):1591–1597.

Jeng JH, Hsieh CC, Lan WH, Chang MC, Lin SK, Hahn LJ, Kuo MYP. 1998. Cytotoxicity of sodium fluoride on

human oral mucosal fibroblasts and its mechanisms. Cell Biol Toxicol 14:383–389.

Keeting PE, Scott RE, Colvard DS, Anderson MA, Oursler MJ, Spelsberg TC, Riggs BL. 1992. Development and characterisation of a rapidly proliferating, well-differentiated cell line derived from normal adult human osteoblast-like cells transfected with SV40 large T antigen. J Bone Miner Res 7:127–136.

Kendall C, Stone N, Shepherd N, Geboes K, Warren B, Bennett R, Barr H. 2003. Raman spectroscopy, a potential tool for the objective identification and classification of neoplasia in Barrett's oesophagus. J Pathol 200:602–609.

Kieswetter K, Scwartz Z, Hummert TW, Cochran DL, Simpson J, Dean DD, Boyan BD. 1996. Surface roughness modulates the local production of growth factors and cytokines by osteoblast-like MG63 cells. J Biomed Mater Res 32:55–63.

Kneipp J, Bakker Schut T, Kliffen M, Menke-Pluijmers M, Puppels G. 2003. Characterisation of breast duct epithelia: A Raman spectroscopic study. Vib Spectrosc 32: 67–74.

Koljenovic S, Choo Smith L-P, Bakker Schut TC, Kros JM, Van der Berge J, Puppels GJ. 2002. Discriminating vital tumor from necrotic tissue in human glioblastoma tissue samples by Raman spectroscopy. Lab Invest 82:1265–1277.

Koss KL, Grubbs RD. 1994. Elevated extracellular Mg2+ increases Mg2+ buffering through a Ca-dependent mechanism in cardiomyocytes. Am J Physiol 267:C633–C641.

Krafft C, Knetschke T, Siegner A, Funk RHW, Salzer R. 2003. Mapping of single cells by near infrared Raman microspectroscopy. Vib Spectrosc 32:75–83.

Maquelin K, Choo-Smith L-P, van Vreeswijk T, Endtz HP, Smith B, Bennett R, Bruining HA, Puppels GJ. 2000. Raman spectroscopic method for identification of clinically relevant microorganisms growing on solid culture medium. Anal Chem 72:12–19.

Maquelin K, Kirschner C, Choo-Smith L-P, Ngo-Thi NA, van Vreeswijk T, Stämmler M, Endtz HP, Bruining HA, Naumann D, Puppels GJ. 2003. Prospective study of the performance of vibrational spectroscopies for rapid identification of bacterial and fungal pathogens recovered from blood cultures. J Clin Microbiol 41:324–329.

Nijssen A, Bakker Schut TC, Heule F, Caspers PJ, Hayes DP, Neumann MHA, Puppels GJ. 2002. Discriminating basal cell carcinoma from its surrounding tissue by Raman spectroscopy. J Invest Dermatol 119:64.

Niknahad H, Khan S, Sood C, O'Brien PJ. 1994. Prevention of cyanide-induced cytotoxicity by nutrients in isolated rat hepatocytes. Toxicol Appl Pharmacol 128:271–279.

Notingher I, Verrier S, Romanska H, Bishop AE, Polak JM, Hench LL. 2002. In situ characterization of living cells by Raman spectroscopy. Spectrosc Int J 16:43–51.

Notingher I, Verrier S, Haque S, Polak JM, Hench LL. 2003. Spectroscopic study of human lung epithelial cells (A549) in culture: Living cells versus dead cells. Biopolymers 72:230–240.

Notingher I, Bisson I, Polak JM, Hench LL. 2004a. In situ spectroscopic study of nucleic acids in differentiating embryonic stem cells. Vib Spectrosc (in press).

Notingher I, Bisson I, Bishop AE, Randle WL, Polak JM, Hench LL. 2004b. In situ monitoring of mRNA translation in embryonic stem cells during differentiation in vitro. Anal Chem (in press).

Omberg KM, Osborn JC, Zhang SLL, Freyer JP, Mourant JR, Schoonover JR. 2002. Raman spectroscopy and factor analysis of tumorigenic and non-tumorigenic cells. Appl Spectrosc 56:813–819.

Perez AL, Spears R, Gutmann JL, Opperman LA. 2003. Osteoblasts and MG63 behave differently when in contact with ProRoot^{TM} MTA and white MTA. Int Endod J 36:564–570.

Prescott B, Steinmetz W, Thomas GJ, Jr. 1984. Characterisation of DNA structures by laser Raman spestroscopy. Biopolymers 23:235–256.

Puppels GJ, de Mul F F, Otto C, Greve J, Robert-Nicoud M, Arndt-Jovin DJ, Jovin TM. 1990. Studying single living cells and chromosomes by confocal Raman microspectroscopy Nature 347:301–303.

Puppels GJ, Olminkhof JHF, Segers-Nolten GMJ, Otto C, de Mul FFM, Greve J. 1991. Laser irradiation and Raman spectroscopy of single living cells and chromosomes: Sample degradation occurs with 514.5 nm but not with 660 nm laser light. Exp Cell Res 195:361–367.

Salih V, Knowles JC, O'Hare MJ, Olsen I. 2001. Retroviral transduction of alveolar bone cells with a temperature-sensitive SV40 large T antigen. Cell Tissue Res 304: 371–376.

Shafer-Peltier KE, Haka AS, Fitzmaurice M, Crowe J, Myles J, Dasari RR, Feld MS. 2002a. Raman microscopic model of human breast tissue: Implications for breast cancer diagnosis in vivo. J Raman Spectrosc 33:552–563.

Shafer-Peltier KE, Haka AS, Motz JT, Fitzmaurice M, Dasari RR, Feld MS. 2002b. Model-based biological Raman spectral imaging. J Cell Biochem 39:125–137.

Smith J, Kendall C, Sammon A, Christie-Brown J, Stone N. 2003. Raman spectral mapping in the assessment of axillary lymph nodes in breast cancer. Technol Cancer Res Treat 2:327–332.

Stone N, Stavroulaki P, Kendall C, Birchall M, Barr H. 2000. Raman spectroscopy for early detection of laryngeal malignancy: preliminary results. Laryngoscope 110: 1756–1763.

Stone N, Kendall C, Shepherd N, Crow P, Barr H. 2002. Near-infrared Raman spectroscopy for the classification of epithelial pre-cancers and cancers. J Raman Spectrosc 33:564–573.

Takai Y, Masuko T, Takauchi H. 1997. Lipid structure of cytotoxic granules in living human killer T lymphocytes studied by Raman microspectroscopy. Biochim Biophys Acta 1335:199–208.

Tarnowski CP, Ignelzi MA, Jr., Morris MD. 2002. Mineralization of developing mouse calvaria as revealed by Raman microspectroscopy. J Bone Miner Res 17:1118–1126.

Thomas GJ, Jr., Hartman KA. 1973. Raman studies of nucleic acids VIII estimation of RNA secondary structure from Raman scattering by phosphate-group vibrations. Biochim Biophys Acta 312:311–322.

Tu AT. 1982. Raman spectroscopy in biology: Principles and applications. New York: John Wiley and Sons.

Uzunbajakava N, Lenferink A, Kraan Y, Willekens B, Vrensen G, Greve J, Otto C. 2003a. Nonresonant Raman imaging of protein distribution in single human cells. Biopolymers 72:1–9.

Uzunbajakava N, Lenferink A, Kraan Y, Volokhina E, Vrensen G, Greve J, Otto C. 2003b. Non-Resonant

confocal Raman imaging of DNA and protein distribution in apoptotic cells. Biophys J 84:3968–3981.
Verrier S, Notingher I, Polak JM, Hench LL. 2004. In situ monitoring of cell death using Raman Micro-Spectroscopy. Biopolymers 74:157–162.
Wergedal JE, Baylink DJ. 1984. Characterization of cells isolated and cultured from human bone. Proc Soc Exp Biol Med 176:60–69.
Wold S, Esbensen K, Geladi P. 1987. Principal components analysis. Chemo Intell Lab Syst 2:37–52.
Wolthuis R, Bakker Schut TC, Caspers PJ, Buschman HPJ, Romer TJ, Bruining HA, Puppels GJ. 1999. Raman spectroscopic methods for in vitro and in vivo tissue characterisation. In: Mason WT, editor. Fluorescent and luminescent probes for biological activity, London: Academic Press.